

**The response of impounded sediment to a culvert
replacement project on Sutter Creek, a tributary of
Honey Grove Creek, in the Alsea River Basin of the
Central Oregon Coast Range**

1.0 Introduction

Purpose of culvert replacement (agencies involved, legislation, acts, etc)

General description and introduction to the study site (refer to details below).

1.1 – Study site

1.1.1 - Physiography

Sutter Creek is a right bank tributary stream of Honey Grove Creek, which is located in the Alsea River Basin in the Central Oregon Coast Range (Figure 1.1). The 0.425 mi² (272 acres) Sutter Creek Basin is entirely underlain by the Tyee Formation, which was deposited during the middle Eocene approximately 28 million years ago (mya), and which is composed of medium- to fine-grained sandstone and siltstones. Igneous intrusions dating from the Oligocene (33.7 to 23.8 mya) are also present underneath the basin (ref). Basin relief ranges from about 390 feet at the confluence of Sutter Creek and Honey Grove Creek to about 1,360 feet in the headwaters. Climate data for the period 1954-2003 from the Alsea Fish Hatchery¹, located about three miles northwest of the basin, indicate a mean annual precipitation of 92 inches per year, with a range between 63 inches and 139 inches. The climax vegetation community in this part of the Coast Range, and which originally covered the entire Sutter Creek Basin, is Douglas Fir (*Pseudotsuga menziesii*).

1.1.2 – Site description and history

1.1.2.1 – Logging history

This coverage of Douglas Fir has been highly disturbed since World War II by logging activity [Kagan, 1992 #1989], and this has had a significant impact on the development of the fluvial system within the basin. Figures 1.2a-g presents a summary of this logging history as determined from a series of Bureau of Land Management (BLM) aerial photographs. The areas within the red lines have either been recently clear-cut at the time the photograph was taken, or are at an early stage of recovery from having been clear-cut. The criterion for determining what constitutes an early stage of recovery involves trying to determine whether the vegetation cover appears to be sufficiently well re-established to prevent significant soil erosion due to overland flow. This is a somewhat subjective and inexact undertaking, especially on the black and white photographs (Figures 1.2a-c), but is sufficient for the current purpose. The results of the analysis show that virtually the entire basin surface area has been clear-cut since 1950, which will have caused large volumes of soil to be eroded from the steep hillslopes (Figure 1.1, Inset A) and transported through the channel network.

1.1.2.2 – Floodplain sediments

Upstream of Honey Grove Road a small floodplain exists on both sides of Sutter Creek that extends and gradually narrows for a distance of several hundred feet upstream to the mouth of a small canyon. It is not known if the floodplain was formed solely by

¹ Data available from <http://www.wrcc.dri.edu/cgi-bin/cliMAIN.pl?oralse>

fluvial processes, solely by lacustrine processes, or by a combination of both, but there is some evidence to suggest the latter. The current elevation of Honey Grove Road is 295.5 feet in the coordinate system used in this study (see Section 2.2 below) and this elevation occurs on the floodplain surface about one-third of the distance from the canyon mouth to the road. Assuming that the bed elevation has not changed significantly since the road was built, then standing water could not have accumulated upstream of the road for more than about two-thirds of the distance from the road to the mouth of the canyon. Therefore the upstream third of the floodplain deposit must be fluvially deposited, while the downstream two-thirds may be combination of both fluvial and lacustrine deposition.

Water is known to have been impounded upstream of Honey Grove Road for at least some of the time since the road was built in the late 19th century², although the precise period or periods of this impoundment and also its historical physical extent are unknown. A pond is visible in Inset A (Figure 1.1), and the aerial photography upon which this map is based dates from 1975-76 [United States Geological Survey, 1985 #1996]. This pond is no longer visible on the 1977 BLM aerial photograph, however, (nor, indeed, on any other of the BLM aerial photos), and this suggests either that the impoundment was a permanent feature between the 1970 and 1977 BLM aerial photography missions, or that it was an ephemeral feature. The latter explanation is the more likely, since the flow in Sutter Creek is very low during the summer months (less than 1 cfs) and probably non-existent in very dry years, and therefore probably incapable of sustaining a small body of standing water, especially if this is able to drain away through a culvert. Instead, the standing water was likely to accumulate during high flow events and to slowly drain away thereafter.

The date on which a culvert was first installed under the road is not known but, according to Mr Sutter, who lived by the creek from the 1940s to the 1990s (Figure 1.1, Inset A), there has been a culvert at the site since at least the 1940s. If this observation is accurate, the culvert that was replaced in the fall of 2002 was certainly not the first to have been installed under the road, since it would have been physically incapable of lasting 50-60 years (Knoll, Pers. Comm.), and could indeed have been the second, third or fourth at the site.

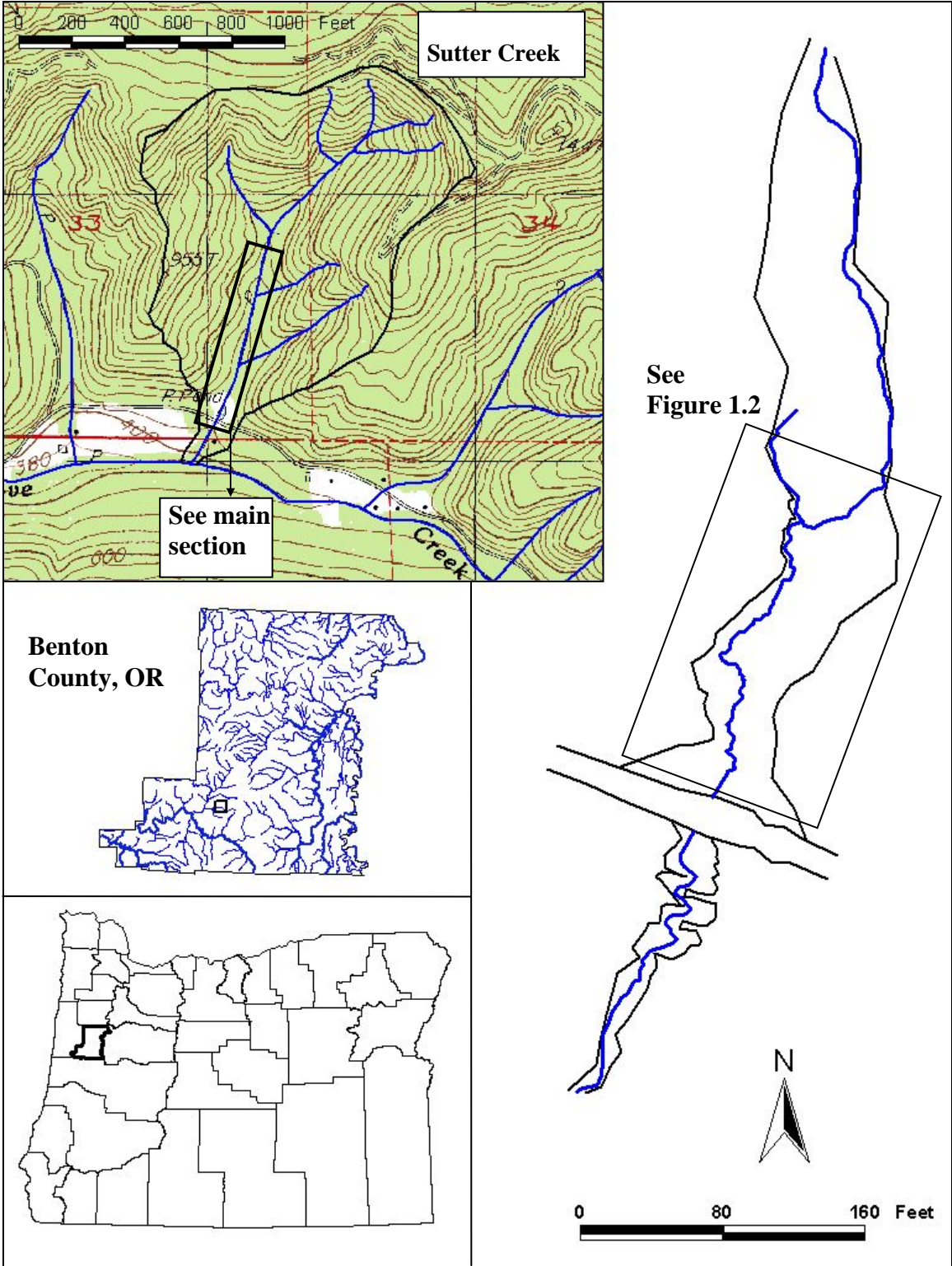
There are a number of possible causes for the impoundment of water upstream of Honey Grove Road and these may have operated separately or in tandem at different times. Historically, there may have been no culvert at the site and water may have simply been allowed to accumulate up to and then to flow over the road surface during high flows. A practice common in the region was to stack large logs in the stream parallel to the flow and to build the road surface across the top of the stack (Sutter or Knoll?, Pers. Comm, 2003). Water would then drain through the gaps between the trunks, although this method is likely to have been very ineffective, since the gaps would clog easily and lead to impoundment. An undersized culvert could also be responsible for backing water up behind the road. The culvert that was removed for this project was four feet in diameter and possibly incapable of passing the highest storm flows, especially if it became partially or fully blocked with sediment and woody debris, of which there is an

² This observation is based on records in the BCPW archive that refer to the road at this time.

abundance within the basin. Beavers were also responsible for the construction of a number of dams in the late 1980s and early 1990s [Sutter, 2003 #1993], which were subsequently removed by BCPW. Unfortunately, there are no records of such maintenance activity in the BCPW archives with which to corroborate this observation, although it does not seem unreasonable since beavers are known to be active in the Coast Range (Grant, Pers. Comm., 2003).

If the aforementioned supposition that the impounded water was only an ephemeral feature during winter high flow events, then this means that at least some of the large volumes of sediment that would have been eroded from the clear-cut areas during storms, would have been deposited once the flowing water entered the impoundment. If the supposition is incorrect or if the drainage through the culvert was good, then sediment would have been primarily deposited on the receding limb of the flood hydrograph.

Understanding the behavior of the system upstream is important in helping to understand how the scour hole developed downstream of the old culvert (Figure ? – *photo of scoured channel downstream*). By impounding water above the elevation of the top of the culvert, a pressure head would develop that would force the water through the culvert as a jet, with the force of the jet being proportional to the depth of water above the culvert top. The jet emerging from the downstream end of the culvert would then have considerable energy with which to scour the channel bed (jet scour refs, eg Bennett, Julien, Stein). Further, if there was a substantial impoundment during high flows, then this may have been capable of trapping a significant proportion of the bed load being transported by the flow. If so, then the water passing through the culvert may have been partially sediment-starved and this may have contributed to the downstream scour. Such an effect is well documented in channels downstream from dams [Williams, 1984 #176].



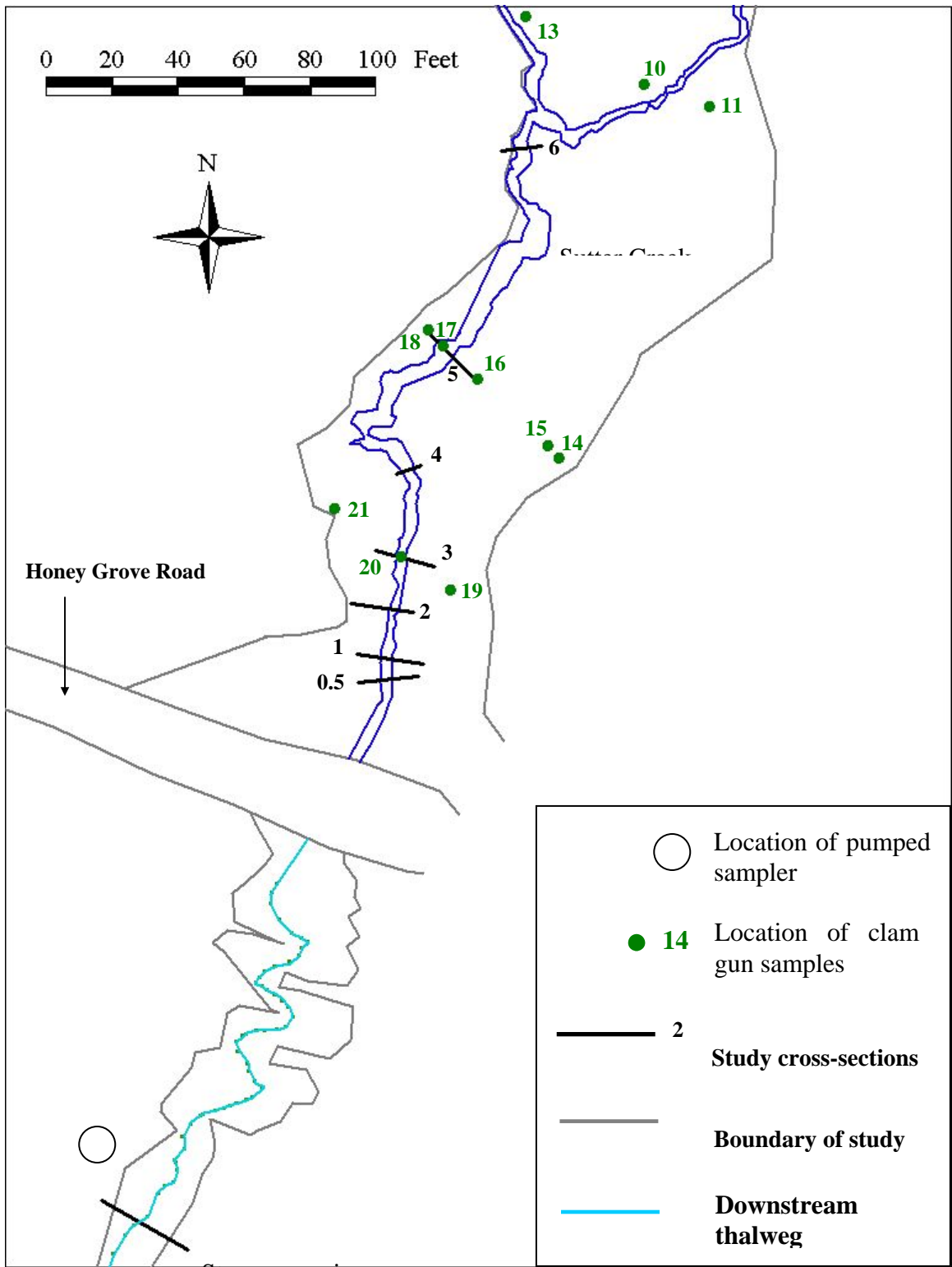
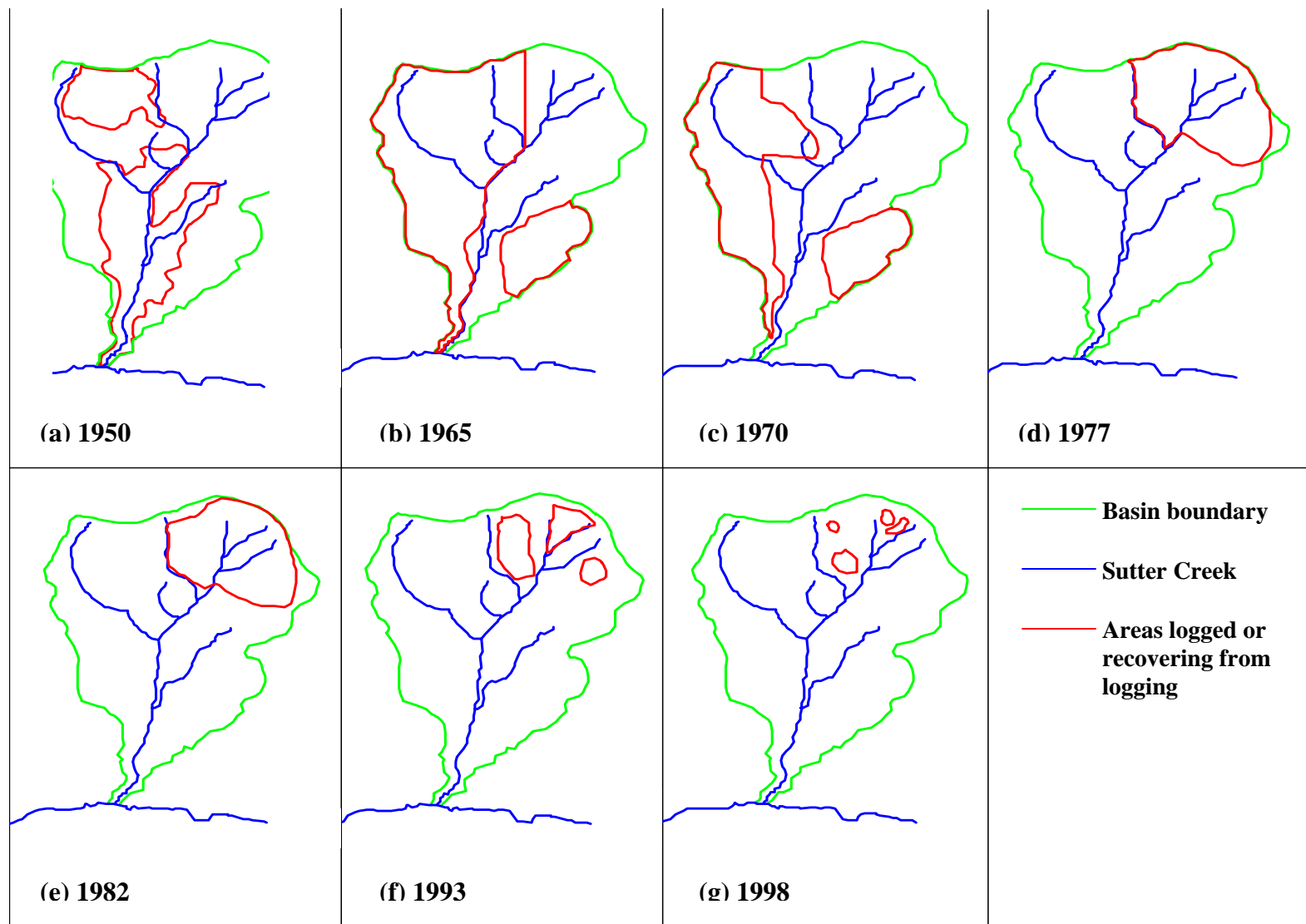


Figure 1.2: Study reach

Figure 1.2: History of logging in the Sutter Creek Basin



1.2 – Theoretical background –*can maybe discuss all this in section 4 in the context of my results in order to avoid repetition.*

1.2.1 – Incising systems

Discussion of the ‘upstream’ aspect of incising channels

The geomorphic concept of convergence states that different processes can result in the same general response [Schumm, 1991 #1023]. Channel incision and the resultant complex response [Schumm, 1977 #1307] can have a number of different causes such as channelization [Simon, 1989 #191; Simon, 1994 #667], the deposition of large volumes of sediment in response to a volcanic eruption [Simon, 1992 #261], and a drop in the baselevel controlling the system [Florsheim, 2001 #619]. It has been suggested that existing models of channel evolution, such as that of [Schumm, 1984 #12] or [Simon, 1989 #191], can be used to describe this response conceptually [Doyle, In press #1425; Harvey, 1986 #226]. For the case of dam removal, in which the incision and complex response of the impounded sediment occurs in response to a drop in the controlling baselevel, this has now been demonstrated using field data for the removal of two *small* dams in Wisconsin [Doyle, 2003 #1424].

Discuss mechanisms of incision, i.e. knickpoints (self-propagating v rotational) versus fluvial erosion over the full length of the affected reach.

Discuss mechanisms of channel widening, i.e. different mechanisms of bank erosion.

Describe how channel evolution models have been used to summarize these changes.

1.2.2 – Downstream response

Movement of sediment through channel system (storage in pools and other slack water environments; dispersive v translational waves – *Tom Lisle’s stuff*. – *don’t bother with this if don’t have time, since downstream is not main focus of study.*

2.0 Field and Laboratory Methods

2.1 – Characterization of floodplain and channel bed sediments

In order to characterize the nature of the floodplain sediments, a series of transects were established across the full width of the impounded sediment surface (Figure 1.2). At several points along each transect, a clam gun was used to extract a core of sediment from either the floodplain or the channel bed. The depth from which a sample could be extracted varied as a function of both the length of the clam gun and the resistance of the material being sampled, with the latter generally being the limiting factor. When resistance became too great, a piece of metal piping was used to probe the sediment to

identify the depth at which a significant change in resistance was encountered. Such a change in resistance was generally the result of a consolidated clay layer. Each core that was extracted from the clam gun was inspected to determine whether there was any stratification of the sediments. Stratification was frequently not very obvious based on a visual inspection but, where suspected based on a textural inspection, the break between the strata was identified in the hole left by the clam gun and its depth measured. A sample of sediment from each stratum was then bagged and labeled in order for a grain size distribution analysis to be conducted.

In a few locations, the clam gun could not be inserted into the channel bed because of the presence of surface gravels. Where this occurred, the surface layer of gravels was scrapped off with a spade and large glass jar (in order to capture the disturbed fines) to the depth of the largest particle in the sampling area (ref) and bagged. A sample of the subsurface sediment was then collected with the glass jar and bagged separately [Bunte, 2001 #256]. The glass jar was also used to collect bulk channel bed samples when the sediment was too liquefied to remain in the clam gun as it was being pulled from the bed.

2.2 - Channel topographic surveys

The evolution of the incising stream network upstream from the new culvert was recorded by repeatedly surveying the channel topography following significant storm events. Table 2.1 summarizes this survey history.

Date	Description of survey
9/6/02	Floodplain, channel banks & thalweg upstream; engineered channel downstream
12/22/02	Channel banks, thalweg & channel bed topography upstream; gauging cross-section downstream
1/8/03	Channel banks, thalweg, channel bed topography & cross-sections upstream; gauging cross-section downstream
2/12/03	Channel banks, thalweg & channel bed topography upstream; gauging cross-section downstream
4/18/03	Channel banks, thalweg, channel bed topography & cross-sections upstream; gauging cross-section downstream

Table 2.1: Survey history

No survey was shot prior to the start of construction activity, since the area immediately upstream and downstream of the road was extensively reshaped by earth moving equipment and such a survey would have produced no meaningful baseline on which to base subsequent geomorphic analyses. The first survey was shot immediately following installation of the new culvert. At this time in early September, flow through the upstream channel network was very low and was insufficient to cause any channel incision. This survey thus characterized the stream network prior to the onset of channel incision and forms the baseline upon which the volumetric analysis and sediment budget is based.

The first survey was shot by a team from Benton County Public Works (BCPW) using a (*inset instrument specification*). A master control point was established on the

upstream half of the road by inserting a piece of survey-capped steel rebar into the road such that its top was about six inches below the road surface. Two other additional control points were also established at this time, one buried in the impounded sediment about x hundred feet upstream of the road and the second on the downstream side of the road and on the edge of the clearing to the left of the channel (Figure 2.1). These control points are not tied in to any national or state coordinate system (Wilson, Pers. Comm, 2003). From the control points in the road and impounded sediment, a series of transects was shot across the entire floodplain surface to capture the breaks of slope between the surrounding slopes, the floodplain and the channel boundary. Additionally, the engineered channel immediately downstream of the culvert was surveyed. This will be surveyed once or twice per year for the next three (*need to check this*) years by BCPW in order to verify its continued stability.

All subsequent surveys were shot by the author using a (*inset instrument specification*). The tops and bottoms of both banks were surveyed longitudinally, as was the thalweg, while additional points were shot as necessary to capture further details of channel bed or bank topography. A series of cross-sections was also surveyed, although less frequently than the channel bed and banks (Table 2.1). The engineered channel downstream of the culvert was not resurveyed, since its stability is not the focus of this particular study.

2.3 – Discharge

Sutter Creek is an ungauged stream, but in order to develop meaningful analyses of the system's evolution, it is critical to know the discharge that is performing the observed geomorphic work. A number of methods exist for transferring flow data from gauged to ungauged sites, such as the drainage area/discharge method [Wahl, 1995 #255] or the use of regional regression equations [Jennings, 1994 #9]. However, a direct measure of discharge is obviously more accurate and, for a small stream like Sutter Creek, relatively easy to obtain.

A continuous estimate of discharge for a site is provided by a stage-discharge, or rating, curve. This involves measuring stage almost continuously and periodically measuring flow velocities across the stream in order to calculate discharge. Ideally these measurements would be collected at a stable cross-section in bedrock or in very coarse sediment so that the relationship between stage and discharge is not altered by the passage of a large flood that mobilizes the channel boundary and alters its cross-sectional shape. Unfortunately, no such site is available at Sutter Creek and so a fairly cohesive, near rectangular cross-section just downstream of the engineered channel was chosen (Figure 2.1). A description of the data collection process is provided below, while the construction of the rating curve is discussed in detail in section 3.3.

2.3.1 – Measurement of stage

Stage was measured at 15-minute intervals using an OM-CP-Level101-SS submersible water level logger produced by Omega Engineering, Inc. The logger was

attached to a chain and lowered into a narrow PVC tube, which was attached to a metal stake hammered into the deepest part of the channel immediately adjacent to the left bank (Figure 2.2 – *photograph of downstream gauging cross-section*). The logger’s sensor was thus resting on the bed at the deepest point in the channel and so provides an accurate record of stage. The logger was periodically downloaded into a laptop computer in the field.

2.3.2 – Measurement of flow velocity

Flow velocity was measured at several measuring verticals across the stream using a Marsh-McBirney (*specification*) electromagnetic flow meter. The number of measuring verticals chosen is the single biggest factor affecting the absolute accuracy of the subsequent discharge calculation [Hersch, 1999 #1245]. The uncertainties associated with this calculation for different numbers of verticals, expressed at the 95% confidence level, are presented in Table 2.2 ([Hersch, 1978 #1634], cited in [Hersch, 1999 #1245]).

Number of verticals	Percentage uncertainty at 95% level
5	20
10	10
15	7
20	5
25	5
30	3
35	3
40	3
45	3
50	3

Table 2.2: Uncertainty in calculated discharge

Over the period in which velocity data were collected, the wetted channel width generally varied between about 4.6 feet and 5.9 feet depending on the stage and, for this range, Hersch (1999) recommends measuring velocity at between five and eight verticals. Velocity was thus initially measured at about 0.8-foot intervals across the channel, which resulted in seven or eight verticals. But Table 2.2 suggests that this might result in an uncertainty of 10% to 15% in the calculated discharge. In order to assess the accuracy of using a smaller number of verticals in the initial site visits, the spacing of verticals in subsequent visits was reduced to about 0.3 feet, which resulted in 17 to 21 verticals depending on stage.

2.4 – Sediment transport

Both bedload and suspended load sediment transport were measured during storm events.

2.4.1 – Bedload transport

Obtaining an accurate measurement of the mass of material moved as bedload in the field is a notoriously difficult undertaking because of the spatial and temporal variation of this movement along the channel bed. The only way to obtain a truly accurate estimate of bedload transport is to use a continuously recording pit-type sampler, as described by [Einstein, 1944b #1260; Garcia, 2000 #1214; Habersack, 2001 #1210; Reid, 1980 #1259]. These devices work through a system of collection bins mounted on pressure pads, which are installed in a trench across the full channel width, such that the top of the bins are flush with the channel bed. As bedload moves it falls into the bins and the subsequent change in pressure is continuously recorded. Utilizing knowledge of the specific gravities of water and the sediment, the rate of sediment transport at different points across the stream can be continuously calculated. Such devices are costly, though, and beyond the scope of this project.

Bedload transport was thus measured using a (*sampler spec.*) Helley-Smith sampler. While this device only allows bedload transport to be measured at one point across the stream bed, its portability compared to the pit-type samplers means that bedload transport can be easily measured at several locations. Bedload samples were thus collected both upstream and downstream of the incising reach (see Figure 2.1 for sampling locations). The mouth of the sampler was placed on the bed of the thalweg and three two-minute samples were collected. These were composited into a ziplock bag and transported to the laboratory in order to undertake a dry sieve analysis.

2.4.2 – Suspended load transport

Suspended sediment was measured at regular intervals using a (*sampler spec.*) ISCO pumped sampler. The sampler can be programmed to collect different volumes of water at different time intervals, which are stored in 24 500-ml plastic bottles in the body of the sampler. The instrument was installed on the right bank downstream of the incising reach with the intake nozzle positioned in the middle of the stream and about 4 inches from the channel bed. This was to ensure that the sampler would suck in as little bedload as possible during sediment-transporting flows but that it would be fully submerged and thus collect the required volume of suspended-sediment-containing water.

The sampler was programmed to collect 250-ml samples every six hours, two samples being composited together into the same storage bottle, such that two 500-ml samples were collected in one 24-hour period.

2.5 – The volume of fine sediment stored in downstream pools

Although the principle focus of this study is the incising channel upstream of the new culvert, it is nevertheless important to have some understanding of how the sediment mobilized by this incision impacts the downstream environment.

Between the downstream limit of the project reach and the confluence of Sutter Creek with Honey Grove Creek, field reconnaissance identified eight pools as being sufficiently large to store potentially large volumes of sediment. In order to undertake a truly quantitative analysis of the transportation and deposition of eroded sediment downstream from the project reach it would have been necessary to measure the volume of fine sediment stored in pools after each significant storm event. Because the method used to measure the volume of fine sediment, that of [Hilton, 1993 #1267], is a time intensive approach, it was beyond the scope of this project to do so. Instead, the volume of all eight pools was measured in November 2002 following the installation of the new culvert but before the first winter rains, and the volume of three of these pools again measured following cessation of the rains in May 2003. A detailed description of the method can be found in [Hilton, 1993 #1267], but a brief summary is provided here.

In order to calculate the dimensionless volume of fine sediment stored in a pool (V^*), it is necessary to measure the volume of water and fine sediment in the *residual pool*, which is defined as the volume of the pool that is below the elevation of the riffle crest at the downstream end of the pool (Figure 2.3 – *scanned copy of Figure 1 from [Hilton, 1993 #1267]*). The first step was to measure the depth of the riffle crest, which is defined as the shallowest continuous line across the channel close to where the water surface becomes continuously riffled, using a graduated copper rod. The depth was estimated as the mean value of about five measured points.

The depth of water and fine sediment was then measured within the *scoured residual pool*, which is the residual pool that would result if all the fine sediment were removed. The lateral boundary of the scoured residual pool occurs where fine sediment depth plus water depth equals the riffle crest depth. Measurements of water and fine sediment depth were then taken at equally spaced points across a series of evenly spaced cross-sections along the pool's length, with zero-area cross-sections assumed at the upstream and downstream ends. Pool lengths were measured by fastening a tape measure between two pieces of rebar inserted into the channel bed at the upstream and downstream ends of the pool, and between two and seven measuring cross-sections were established perpendicular to this tape. The distance between cross-sections was found by dividing pool length by the number of cross-sections chosen for that pool. The position of the first measuring cross-section was found using the random number generator on a calculator and expressing this number as a percentage of the distance between cross-sections. The distance between depth measuring points was determined by choosing between seven and 20 points at which to measure depth at the widest cross-section, and dividing this width by that number of points. The position of the first point was found as described above using the random number generator. Measurements of water and fine sediment were then taken at each point by inserting the graduated rod through the fine sediment until the rod struck the surface of the coarser material forming the boundary of the scoured residual pool.

2.6 – Laboratory sediment analysis

2.6.1 – Dry sieving of floodplain, channel bed and bedload transport samples

All the bedload transport samples and the coarse channel bed and floodplain clam gun samples were dry sieved according to the procedure outlined in *reference*. The samples were washed in a 63- μm sieve in order to separate the fine from the coarse fraction. The turbid washing water was retained and oven dried at ?°C until only the dry fine sediment remained, which was then weighed. The remaining coarse fraction was oven dried overnight at ?°C, weighed and dry-sieved. The sieves used were *sieve spec.* sieves ranging from numbers ? to ? (? inches to ? inches). Each sample was sieved for 10 minutes and the fraction retained on each sieve weighed.

2.6.2 – Determination of suspended sediment concentration

The suspended sediment concentration was determined according to the procedure outlined in *reference*. A ?-ml sub-sample of each 500-ml composite sample was.....

3.0 Data Analysis and Results

3.1 - Characterization of floodplain and channel bed sediments

Put discharge analysis next, then channel evolution, then sediment analysis, then pool volumes.

3.2 – Upstream channel evolution

To quantify the impact of installing the new culvert on the upstream system, the survey data can be used to perform both two-dimensional and three-dimensional analyses of channel evolution.

3.2.1 – Two-dimensional analysis - channel geometry

3.2.1.1 – Bed slope

The channel thalweg, the deepest portion of the streambed, was surveyed over a stream centerline distance of just under 200 feet upstream from the upstream end of the new culvert. These channel bed profiles are presented in Figure 3.4. (Please note that when specific sections of the profile are being discussed, they will be referred to by their northing coordinates). The first survey, carried out by the BCPW survey team, was shot at a much lower spatial resolution than the subsequent surveys but nevertheless still provides a good idea of the channel profile prior to the onset of the winter high flow events (Figure 3.4).

The first two surveys show a significant drop in bed elevation, of up to two feet in some places, over almost the full length of the study reach during the first winter high flow event from the 14th - 19th December 2002 (Figure 3.9). The second and third surveys show a further decrease of smaller magnitude during the second high flow event from the 26th December to the 7th January 2003 (Figure 3.9). With the passage of a further four high flow events (Figure 3.9), however, the bed elevation appears to remain essentially stationary along virtually the entire study reach, with only minor oscillations at various locations along the profile (Figure 3.3).

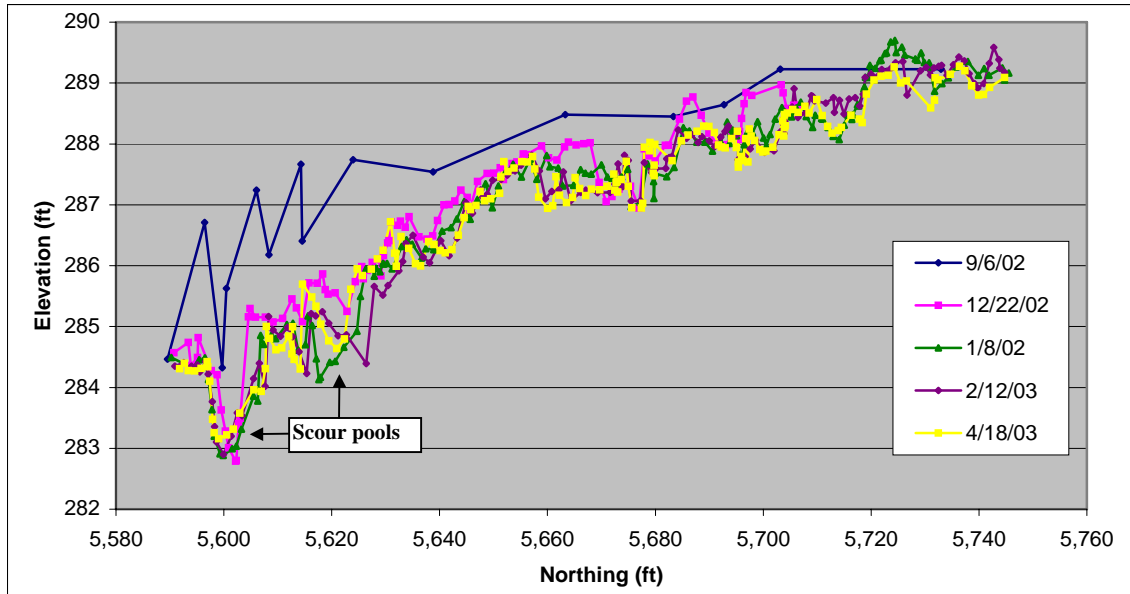


Figure 3.4: Longitudinal profiles of the channel bed through the incising reach

This behavior is shown much more clearly in Figure 3.5. All the surveys show a significant break in slope at about 5,655 feet (Figure 3.4). By splitting each survey's data into two groups at this point and fitting a linear line-of-best-fit through them, the mean bed elevations and mean slopes of the upstream and downstream sections are obtained (Figure 3.5). There are only very minor adjustments to bed elevation and slope in the downstream section between the third and fifth surveys. Similarly, in the upstream section, there is virtually no change between the third and fourth surveys, and only a further small drop in mean elevation in the upstream half of the section between surveys four and five.

Figure 3.5 also reveals interesting information regarding the mechanisms of bed elevation change and slope adjustment. In the downstream section, the magnitude of change of bed elevation between the first and third surveys is essentially uniform along the entire section, *i.e.* there is very little change in slope as the elevation decreases (Table 3.1, Figure 3.6). Conversely, between the first and fourth surveys in the upstream section, the greatest drop in bed elevation occurs near cross-section four (5,665 feet) and there is virtually no change in elevation by about 5,740 feet. The bed is thus pivoting downwards about this point, causing slope to increase (Table 3.1, Figure 3.6).

The dominant mode of vertical adjustment along the entire downstream section thus appears to be fluvial erosion during high flow events. This erosion appears to propagate into the upstream section where it essentially ceases at 5,735 feet (Figure 3.5). Although there are many small steps in the long profiles that are suggestive of knickpoints (Figure 3.4), field observations indicate that these steps are formed by logging debris and root networks that are gradually becoming exposed as the channel incises (Figure ? include a photograph to provide an example of this). This woody material acts to focus the flow and cause local scouring of the channel bed, which results in a feature morphologically similar to a knickpoint but whose mechanism of formation is

different to that of a knickpoint. Furthermore, there is no evidence from the thalweg profiles that these steps migrate upstream, which would be expected if they were knickpoints.

Further evidence to support the theory of fluvial erosion as opposed to knickpoint migration comes from the stratification of the channel bed deposits. Analysis of these deposits shows that prior to the onset of winter high flows, there was a layer of fine, relatively unconsolidated, material lying on the channel bed (*refer back to relevant section of report – try to present an estimate of the shear stresses that would be required to erode these cohesives (maybe take figures from Andy Simon and Greg Hanson’s jet testing work) and compare these to the shear stresses exerted on the bed as calculated from the current velocity and flow depth measurements – could maybe plot up a graph of shear stresses versus flow depth or discharge for each gauging cross-section to see what discharge, for a given channel width, would be required to generate the shear stresses required for erosion*), which was gradually flushed through the system by the first few high flow events (*refer here to the sediment transport results that should show higher levels of, especially, suspended sediment transport*). Once these fines were flushed away the channel encountered the much more resistant clay layers, which effectively prevented any further channel incision from occurring. The point where incision ceases at around 5,735 feet (Figure 3.5) is also the point where the cohesive material is naturally exposed at the channel bed. It thus appears that any upstream-migrating incision ‘founders’ against this erosion resistant layer.

Discuss the relationship between the end of incision and the onset of lateral adjustment.

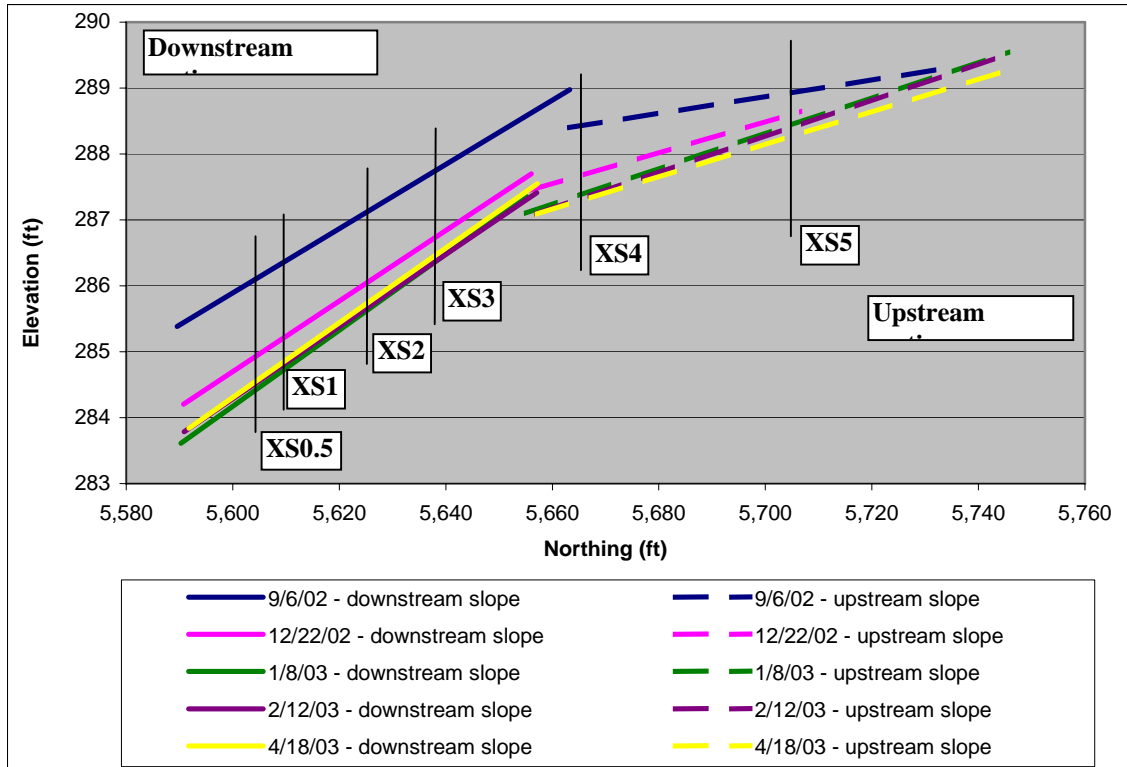


Figure 3.5: Mean bed slopes through the incising reach. (XS = cross-section).

Survey	Mean downstream slope				Mean upstream slope				Slope difference between upstream and downstream sections
	Value	Change	% change	Rate of change (%/?)	Value	Change	% change	Rate of change (%/?)	
9/6/02	0.0488				0.0129				0.0359
12/22/02	0.0534	0.0046			0.0239	0.011			0.0295
1/8/03	0.0577	0.0043			0.0272	0.0033			0.0305
2/12/03	0.0548	-0.0029			0.0275	0.0003			0.0273
4/18/03	0.0567	0.0019			0.0249	-0.0026			0.0318

Table 3.1: Summary of mean bed slope statistics for the incising reach

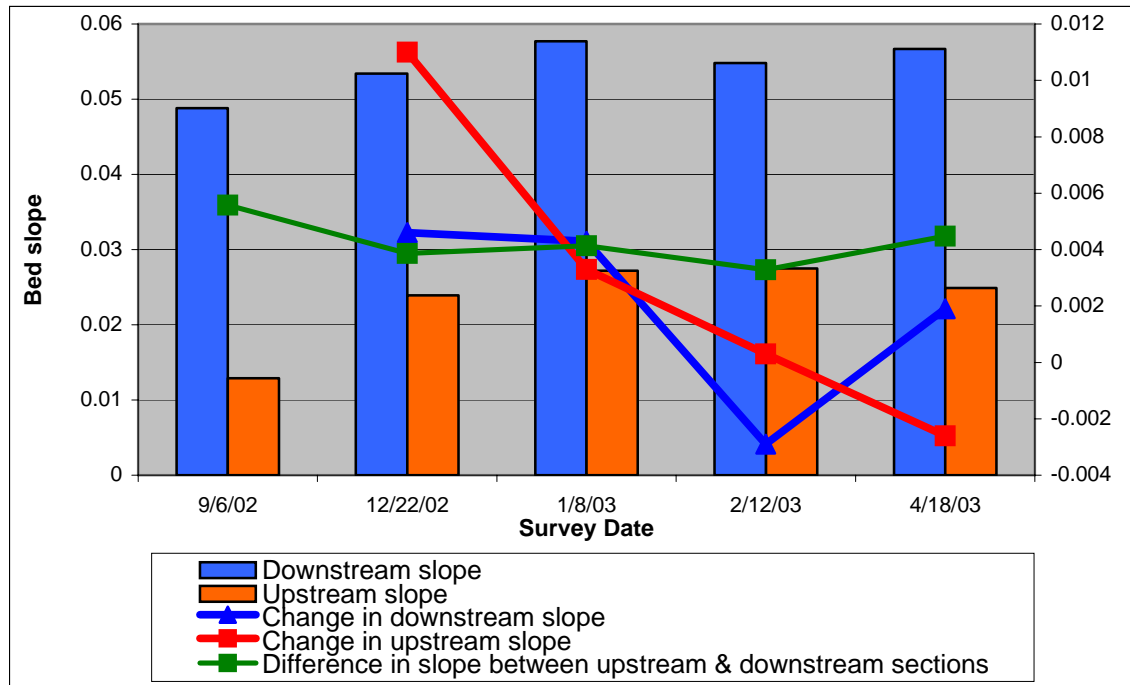


Figure 3.6: Mean channel bed slopes and changes in slope through the two sections of the incising reach

Rate of change of slope. In order to do this will need to estimate a length of time over which morphological work is occurring during each storm and then assume that this rate is occurring constantly over the period of time that work is being done.

3.2.1.2 – Cross-sectional analysis

The active channel bank top width is defined as the horizontal distance between the points along the cross-section at which there is a significant break in slope between the nearly vertical slope of the channel banks and the nearly horizontal floodplain surface. The transition between the two is generally curved, as opposed to being a sharply defined angle, and relocating the precise point that is defined as the bank top from survey to survey is difficult. As a result, a small amount of survey error, of the order of a few inches, is introduced into the survey data. The thalweg is defined as the deepest portion of the channel bed. Both these variables are clearly visible in Figure 3.3.

The channel cross-sections were surveyed less frequently than the channel bed and banks. However, because the density of points in the bank top surveys is so high, it was possible to reconstruct the active channel widths for most surveys by measuring the distance between the bank lines at each cross-section (Figure 3.?) in ArcView. In this way, the record of active channel bank top widths was spatially and temporally extended to allow a more thorough analysis of the adjustment of channel geometry. This methodology was not applied to the data from the first survey, except at cross-section three where the surveyed points fell on the cross-section itself, since the density of bank top points was much lower and did not capture every change in channel bank line direction. The record of thalweg elevation was spatially and temporally extended in a

similar fashion. Where a point from the longitudinal thalweg surveys fell on a cross-section it was added to the record of bed elevation change (Figure 3.2).

For the purpose of describing channel width adjustments, the stream can again be divided into an upstream and downstream section whose boundary is a point about 10 feet upstream of cross-section 3 (Figure 3.?). Interestingly, this point is only about 10 feet downstream from the break in slope at 5,655 feet, which suggests that the steeper slope of the downstream section (Figures 3.4 & 3.5) is exerting a strong influence on the channel width adjustments (*the system cannot reduce its energy by decreasing its slope because the underlying bed material is too cohesive and the survey data have shown that the bed elevation is decreasing uniformly over the full reach of the downstream section. It is thus forced to try to equilibrate by adjusting laterally, which is causing it to scour and undermine the lower sections of the cohesive banks. In turn, this is leading to cantiliver failures (use colin's field reconnaissance book and other thorne refs for mechanisms of bank erosion here) and event-driven channel widening.*

In the upstream zone, field observations and cross-sections four to six (Figure 3.1) show that there has been virtually no change in active channel width. Because the channel boundary material is cohesive, the banks can only retreat through a combination of fluvial scour of the lower bank and subsequent mass wasting of the upper bank, and the only location at which this was observed was between surveys 3 and 4 at cross-section 4. All the other changes shown for these cross-sections are due to survey error discussed above.

Survey error is also inherent in the data from cross-sections 0.5 to three in the downstream zone. It is small, however, compared to some of the observed changes in bank top width. Cross-sections 0.5, one, two and three show increases of 3.4 feet, 2.4 feet, 0.7 feet and 4.7 feet respectively between the second and fifth surveys (Figure 3.1). The spatial distribution of the rate of change of channel width is significant. At cross-section 0.5, the maximum rate of change occurs between surveys two and three and decreases thereafter. At cross-section one the rate of change is essentially continuous throughout the survey period, while at cross-section three there is no change in channel width until survey three, at which point it more than doubles over the course of one high flow event before increasing more slowly from survey four to five. Cross-section two also shows a constant rate of width increase. The total change is much less than at the other three cross-sections, however, and this is due mainly to the presence of a large tree trunk embedded in the left bank (Figure 3.?).

Describe the width and depth trends through time and with increasing distance upstream. Relate the width changes to the changes in depth (and slope), and also influence of woody material.

Estimate rates of change once have worked up sediment transport data and can determine approximately how long geomorphic work (i.e. significant sediment transport) was occurring during each storm event.

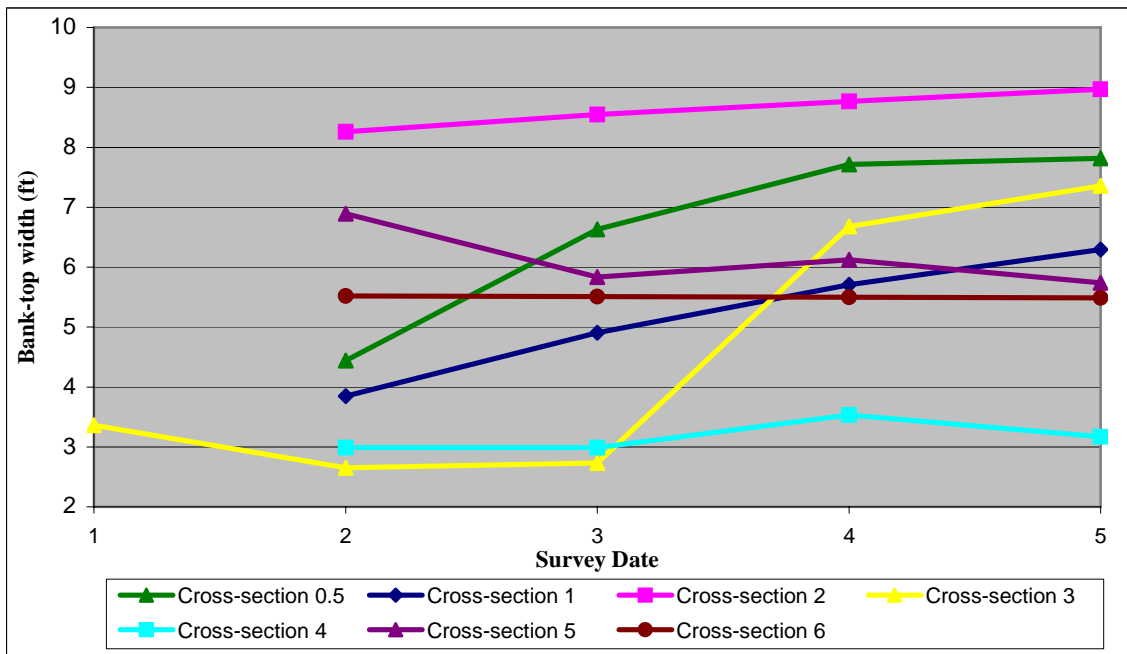


Figure 3.1: Active channel bank top widths

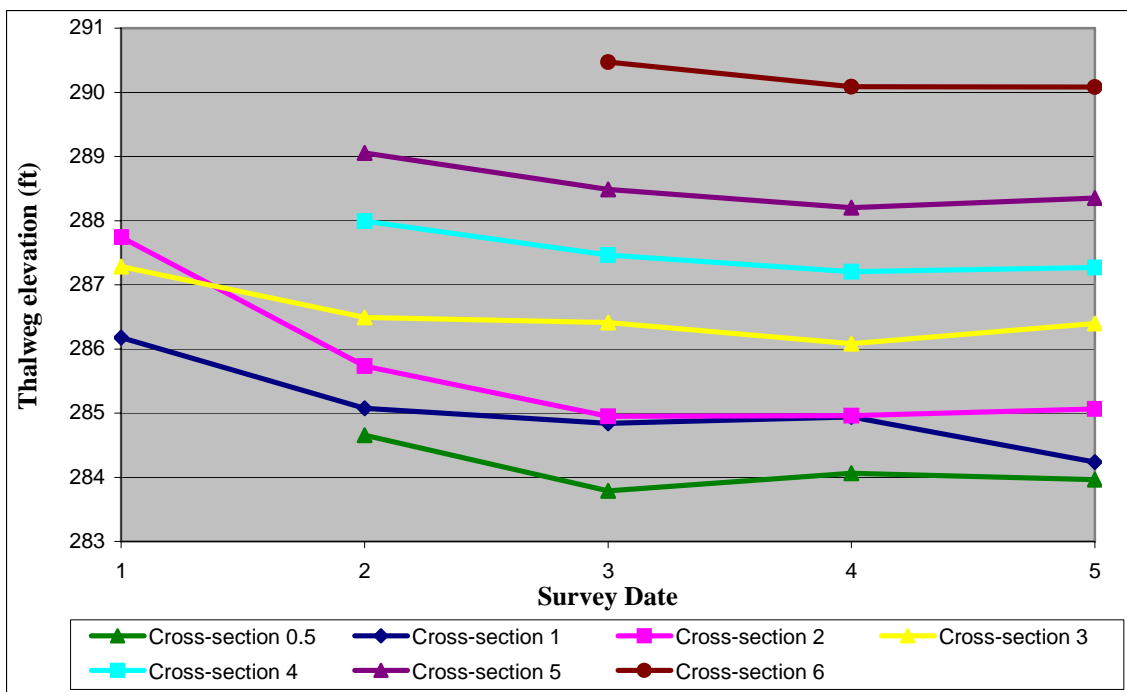


Figure 3.2: Thalweg elevations

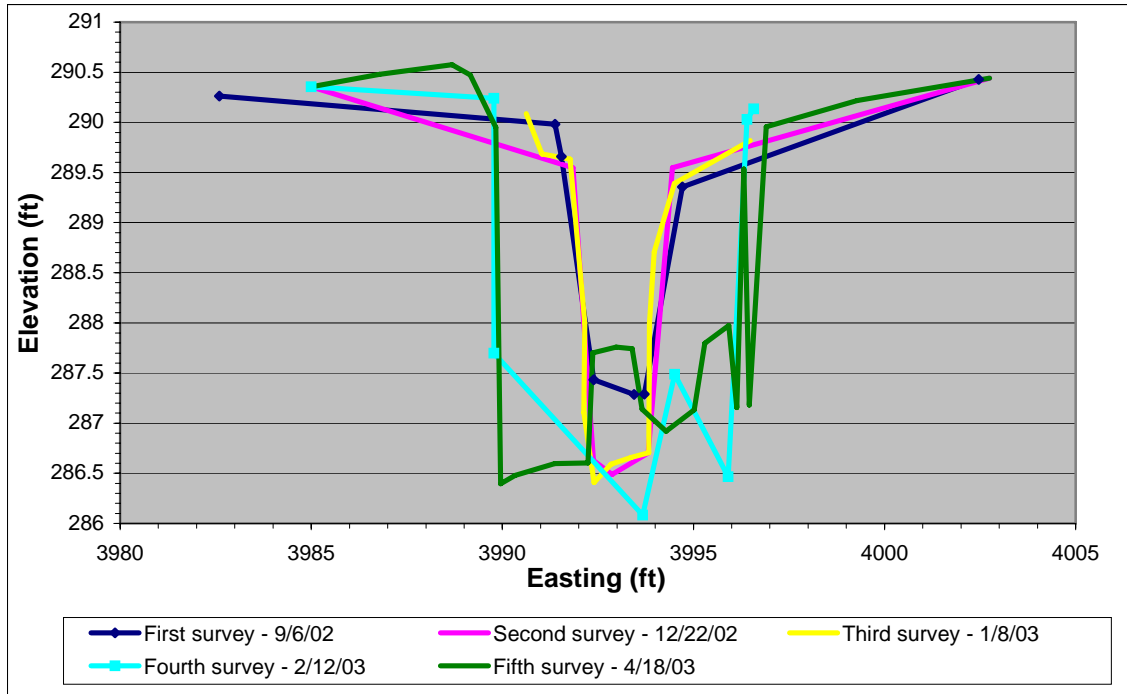


Figure 3.3: Cross-Section Three

Rate of change of width and depth as for Elwha drawdown. In order to do this will need to estimate a length of time over which morphological work is occurring during each storm and then assume that this rate is occurring constantly over the period of time that work is being done.

3.2.2 – Three-dimensional analysis – sediment volumes

3.2.2.1 - Volumetric analysis in ArcGIS

In order to quantify the volume of sediment that was eroded within the upstream channel network, it was necessary to create a three-dimensional surface for each set of survey data. Each surface was then subtracted from the previous survey's surface in order to calculate the net volume of erosion and deposition that occurred within the study reach. This was done by importing the survey data into the 3D Analyst extension to ArcGIS. An Advanced Machine Language? (AML) program¹ was then used to automate the process of surface creation and the subsequent cut and fill analysis. The complete AML is contained in Appendix 1 at the back of this report.

3.2.2.2 – Construction of sediment budget

Table 3.1 and Figure 3.7 provide a summary of the volumetric data produced by the 3D Analyst.

¹ The AML used for this analysis was originally written by Greg Stewart of the Geosciences Department at Oregon State University. The filenames in the original version were simply changed to reflect the names of the data files used in this study.

Surveys analyzed	Volume eroded (ft ³)	Volume deposited (ft ³)	Net volume transported out of reach (ft ³)
1 st & 2 nd	1,169	702	467
2 nd & 3 rd	1,237	374	863
3 rd & 4 th	523	795	-272
4 th & 5 th	1,163	915	247

Table 3.1: Summary of data produced by volumetric analysis

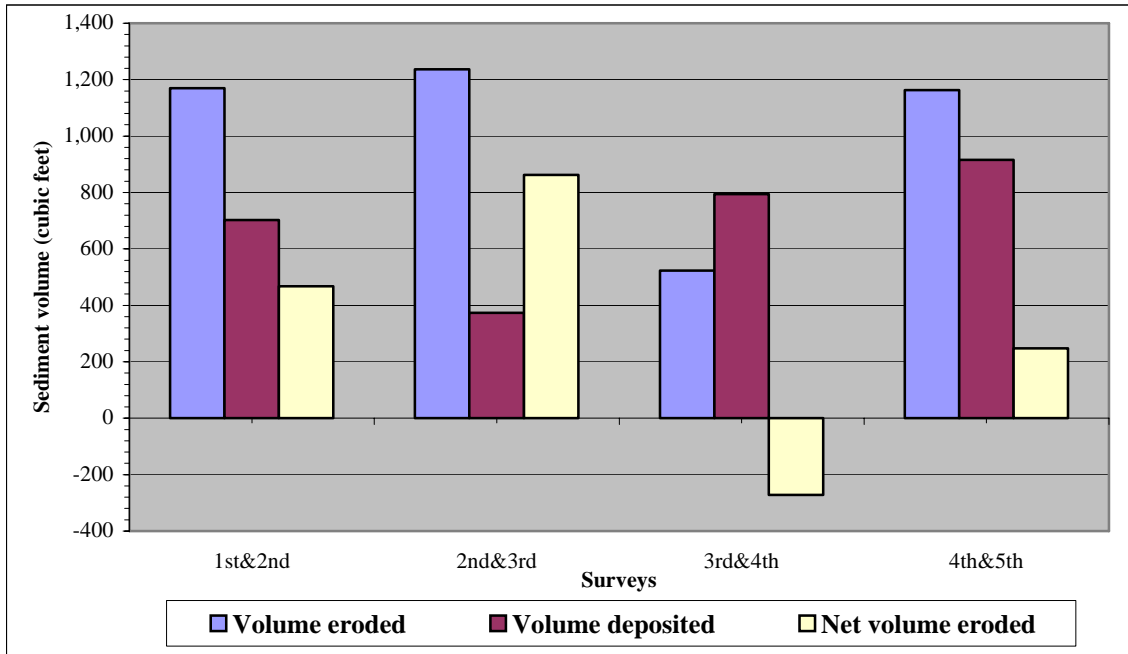


Figure 3.7: Sediment budget for Sutter Creek upstream from the new culvert

When performed at the spatial resolution of the entire study reach, the analysis can only show the net response of the entire reach and not the changes that occur through time in individual reach sections. Nevertheless, when coupled with the two-dimensional results presented above, this net volumetric analysis still yields important information describing the system's evolution.

3.3 – Discharge

The construction of the discharge record that has performed the observed geomorphic work at Sutter Creek is described below. Essentially, this involves developing a relationship between measured discharge and the channel stage at the time that these data were collected, and applying this relationship to the continuous record of stage in order to develop a continuous record of discharge.

3.3.1 – Correction of stage data from the water level logger

The OM-CP-Level101-SS water level logger used to provide a continuous (at 15-minute intervals) record of stage (see section 2.3.1) actually records the total pressure, in inches of water, exerted by the water in the channel and the atmosphere above it. In order to correct these data for atmospheric pressure it is thus necessary to have a continuous record of atmospheric pressure at the site. Unfortunately, an atmospheric pressure logger was only available to the study for a very short space of time. The instrument used was a baroTROLL, produced by In-Situ Inc. and loaned to the study by David Rupp of the Bioengineering Department at Oregon State University. The instrument was installed at the site from the 13th to the 19th March 2003 and set to record at 15-minute intervals, starting on the hour. These intervals coincided with those of the water level logger.

In order to extend the record of atmospheric pressure at Sutter Creek to cover the full period of record of the water level logger (December 12th 2002 to June 2nd 2003), a relationship was developed between atmospheric pressure at Sutter Creek and the Hatfield Marine Science Center (HMSC), Newport, Oregon (Figure 3.2), the nearest site for which historical 15-minute data are available¹. This relationship is described by equation (3.1) and has an R^2 of 0.9337. The equation of the regression line (equation 3.1) was then applied to the pressure data from HMSC to develop an estimate of the pressure at Sutter Creek for the period of record.

$$p_{aSCHg} = 0.9331 * p_{aHMSCHg} + 1.645 \quad (3.1)$$

where p_{aSCHg} = atmospheric pressure at Sutter Creek (inches of Hg)
 $p_{aHMSCHg}$ = atmospheric pressure at the HMSC (inches of Hg)

Because atmospheric pressure is recorded in inches of mercury (Hg), it is necessary to convert this pressure into inches of water. The conversion coefficient varies slightly with the temperature of Hg (*i.e.* with the ambient air temperature), so a linear relationship was developed between the temperature of Hg at 39.2°F (4°C) and at 60°F (15.56°C) (Figure 3.3, equation 3.2). Air temperature was not recorded at Sutter Creek and so was approximated using the air temperature from HMSC², which was also recorded on the

¹ These data were downloaded from <http://hmsc.oregonstate.edu/weather/archives/guinlib/>.

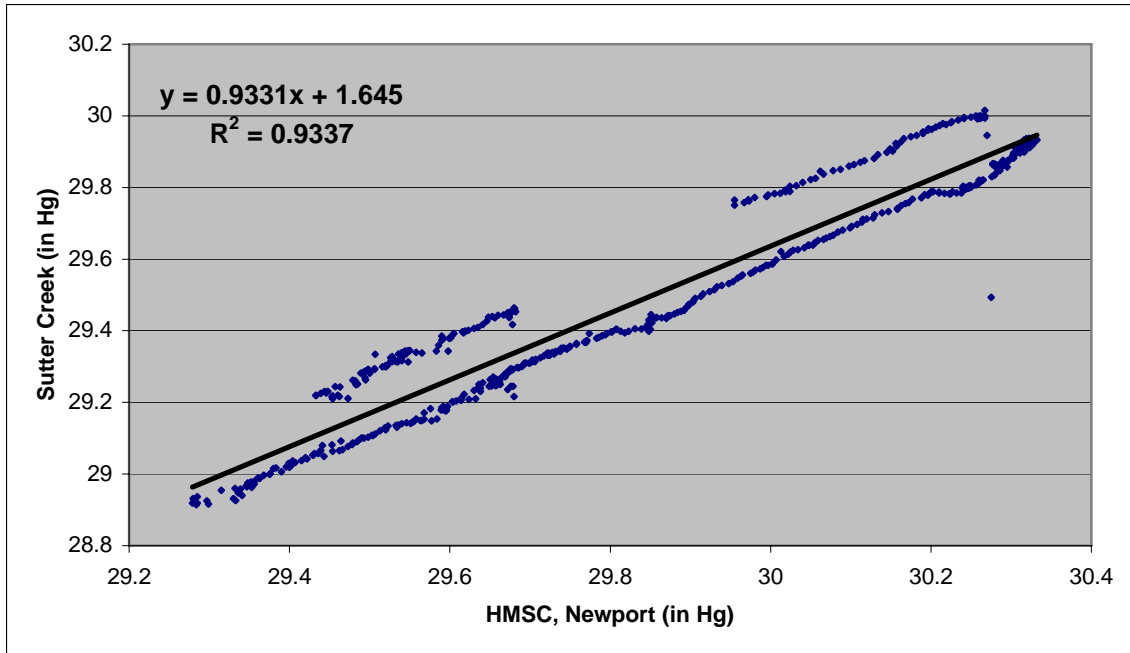


Figure 3.2: Relationship between atmospheric pressure at Sutter Creek and the HMSC, Newport, OR

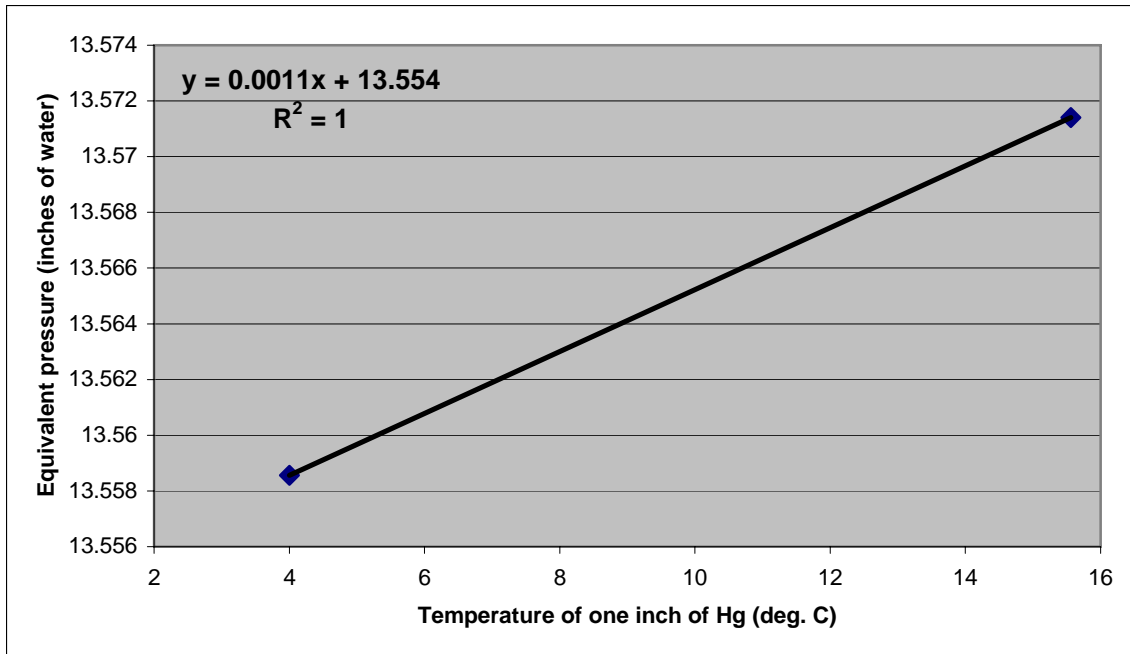


Figure 3.3: Relationship between the temperature of one inch of mercury and the equivalent pressure expressed in inches of water.

same 15-minute intervals as atmospheric pressure at HMSC. This approach is justified since the calculated pressures in inches of water vary by only 12-thousandths of an inch over the range of Hg (air) temperatures (Figure 3.3).

$$p_{aSCH20} = 0.0011 * T_{airHMSC} + 13.554 \quad (3.2)$$

where p_{aSCH20} = atmospheric pressure at Sutter Creek (inches of water)
 $T_{airHMSC}$ = air temperature at HMSC (°C)

To obtain the final, adjusted water depth in Sutter Creek, the products of equations 3.1 and 3.2 were multiplied together for each data point and subtracted from the unadjusted water level recorded by the water level logger (Figure 3.4).

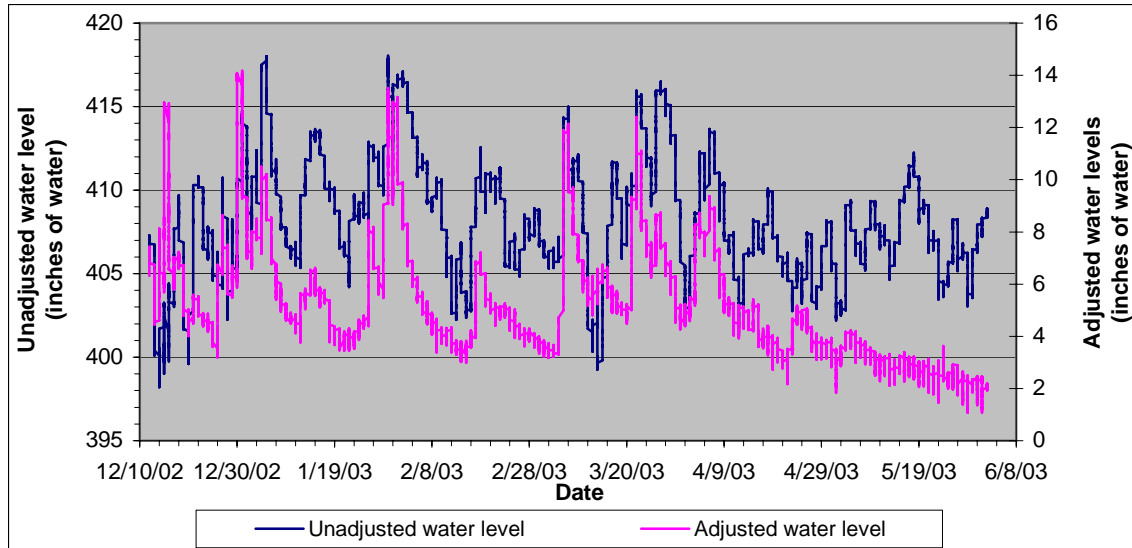


Figure 3.4: Adjusted and unadjusted water levels in Sutter Creek

3.3.2 – Calculation of discharge

Discharge is calculated as the product of flow depth, distance between the measuring verticals and flow velocity, using one of two methods: the mid-section method or the mean-section method. In the former, the velocity measured at a vertical represents the mean velocity for a section, which extends from half the distance to the previous vertical to half the distance to the next vertical. In the latter, the mean velocity of a section is the mean of the velocities at the two adjacent verticals [Hersch, 1999 #1245]. There is no overall advantage to either method in terms of the accuracy of the calculated discharge [Hersch, 1999 #1245] and the mean-section method was used in this case. The discharge passing through each section is calculated using equation (3.3) and then summed with the other section values to determine the overall discharge for the channel.

$$\textit{Inset eq. 2.8 from Herschy (1999).} \tag{3.3}$$

3.3.3 – Development of the rating curve & of the full discharge record

The discharge values calculated in section (3.3.2) were plotted against the corrected stage readings (Table 3.2), with a third-order polynomial expression providing the best fit to the data (Figure 3.5, equation 3.5). Prior to fitting this curve, two suspected outliers were removed from the graph and this markedly improved the R^2 value. Equation (3.5) was then used to recreate the hydrograph through Sutter Creek for the full period of time over which stage data were collected (Figure 3.6).

$$Q = (-27.75 * h^3) + (61.223 * h^2) - (26.348 * h) + 3.4747 \tag{3.5}$$

where Q is discharge in cubic feet per second and h is water depth in feet.

Date of Stream gauging visit	Median time of gauging period	Adjusted water level readings (ft)	Calculated Discharge (cfs)
12/16/02	13:00	0.704	6.494
12/23/03	15:00	0.38	0.789
12/31/02	10:15	0.998	10.215
1/30/03	12:30	1.098	11.813
1/31/03	15:30	0.819	8.353
2/14/03	11:45	0.292	0.494
2/17/03	13:30	0.44	1.289
3/7/03	14:45	0.81	6.937
3/14/03	12:30	0.504	2.312
3/21/03	15:30	0.591	3.228
3/23/03	16:30	0.725	5.521
4/23/03	19:15	0.346	0.331

Table 3.2: Summary of rating curve variables

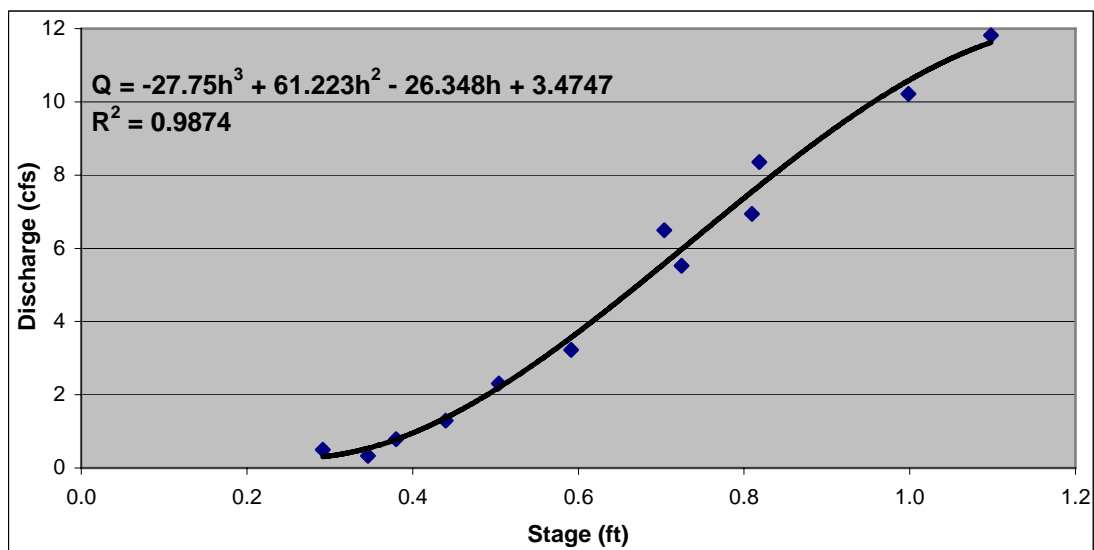


Figure 3.5: Rating curve for Sutter Creek

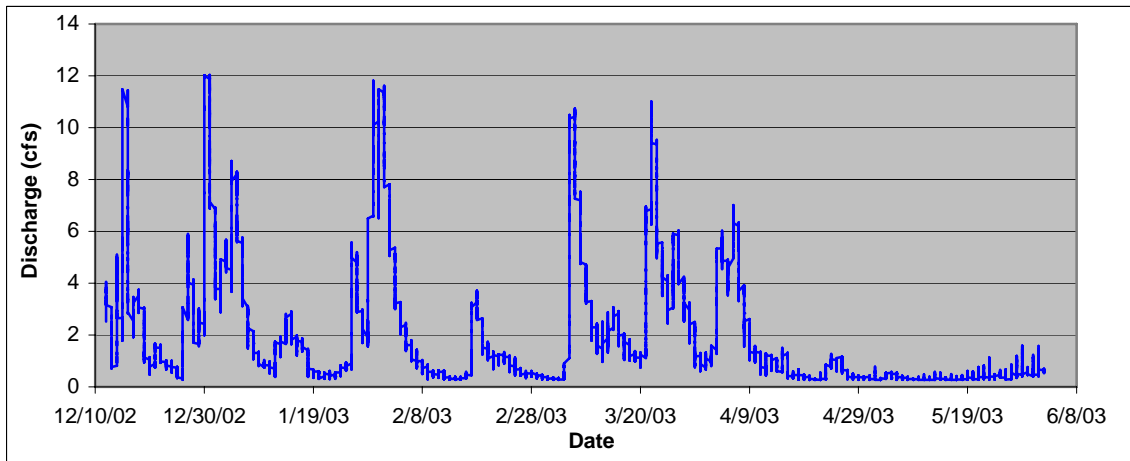


Figure 3.6: Hydrograph for Sutter Creek composed of 15-minute-interval discharge estimates

Need to include graph showing downstream cross-sections and explain that there has been no significant change in the cross section and therefore that there is no significant error in the rating curve due to a change in the stage-discharge relationship.

3.4 – Sediment analysis

3.4.1 – Characterization of floodplain and channel bed samples

The floodplain sediment cores were collected in a series of four transects moving downstream through the study area (Figure 1.2). If these transects are numbered one to four in the downstream direction, then points 8 and 9 are transect one, points 10 to 13 transect two, points 14 to 18 transect three and points 19 to 21 transect four. The grain size distribution plots for each channel bed sample and each floodplain sediment strata are presented in Appendix B.

Comparison of points eight, 12 and 18 (Figure 3.12, Table 3.3), which are all located down the right side of the study area, shows a clear decrease in the D_{50} ¹ of the surface samples, and of the D_{50s} of the second and third depth increments² from point 8 to point 12. Points 8 and 12, with the exception of the second depth increment at point 12, also show a strong coarsening of the D_{50} towards the floodplain surface. Unfortunately, many of these samples do not show a value for D_{50} , which occurs because the D_{50} in these cases is finer than can be detected by the dry sieve analysis (0.002 inches or 0.053 mm). (In order to measure the grain size distribution of the silt and clay fraction it would have been necessary to carry out a pipette analysis, which was beyond the financial scope of this project). The pattern of downstream fining and upwards coarsening suggested by the D_{50} data is replicated and reinforced by the D_{84} data (Figure 3.13, Table 3.3). The D_{84s} of the first and second depth increments of points 8, 12, 18 and 21, and the third depth

Point No.	Depth of sample strata (feet)	D_{50} (in)	D_{84} (in)
7	Pool bulk sample	0.014	0.11
8	0 - 0.85	0.011	0.12
8	0.85 - 1.21	0.0062	0.015
8	1.21 - 2	0.0094	0.097
8	2 - 2.49	0.0084	0.15
9	0 - 1.15	0.003	0.009
9	1.15 - 1.38	None	0.0082
10	Streambed bulk sample	None	0.0035
11	0 - 1.18	0.003	0.013
11	1.18 - 1.38	None	0.0042
12	0 - 0.43	0.0068	0.019
12	0.43 - 1.61	0.0052	0.012
12	1.61 - 2.03	0.0034	0.008
13	Streambed bulk sample	None	0.0052
14	0 - 0.39	None	0.0027
14	0.39 - 1.25	None	0.0028

¹ The D_{50} is the median grain size of the grain size distribution, while the D_{84} is the grain size which 84% of the sample is finer than.

² Please note that these increments are not of equal depth at each sample point. The depths of each data point referred to in Figures 3.12 and 3.13 can be obtained from the legends of Figures B1a-j in Appendix B.

15	Streambed bulk sample	None	0.01
16	0 - 0.39	None	0.0062
16	0.39 - 0.89	None	0.0037
16	0.89 - 1.41	None	0.0042
17	Streambed armor layer	0.4	0.8
17	Streambed subsurface 1 bulk sample	0.0086	0.16
17	Streambed subsurface 2	0.0021	0.0033
18	0 - 0.26	0.0024	0.024
18	0.26 - 0.92	None	0.015
18	0.92 - 1.67	None	0.0068
19	0 - 0.46	None	0.0024
19	0.46 - 0.79	None	0.003
20	Streambed bulk sample	0.0041	0.028
21	0 - 0.69	None	0.0032
21	0.69 - 1.18	None	0.0028

Table 3.3: D_{50} & D_{84} of floodplain and channel bed sediment samples

increments of points 8, 12 and 18, all down the right side of the study area (Figure 1.2), show a decrease in the downstream direction. Point 18 is a slight anomaly in that it is a little coarser than point 12 upstream, but the overall trend is still suggestive. This pattern also occurs, albeit less strongly, down the left side of the study area, with the first depth increment of points 11, 14 and 19, and the second depth increments of points 9, 11 and 14 (Figure 1.2) all showing downstream fining. Points 9, 11, 12, 16, 18 and 21 also all show a coarsening towards the floodplain surface.

The D_{50} and D_{84} data thus show strong trends of downstream fining and upwards coarsening, which are more pronounced down the right side of the study area than the left. This pattern is strongly indicative of a floodplain that has been formed by sediment deposition in standing water (ref Morris?, Elliott, 1978?). If the floodplain had been formed by fluvially-driven lateral or vertical accretion processes, then the D_{50} and D_{84} data would have shown a trend of upwards *fining* [Knighton, 1998 #1862]. There is also a strong fining trend from right to left across the floodplain. All points across transects one, two and three show this trend at each depth increment (Figure 3.13). This suggests that the current was generally directed towards the right side of the study area as it entered the impoundment, thus creating a higher energy environment that prevented the deposition of the finest fractions of the sediment load. Conversely, the left side of the study area would have been a generally lower energy environment in which these fines would have been able to deposit.

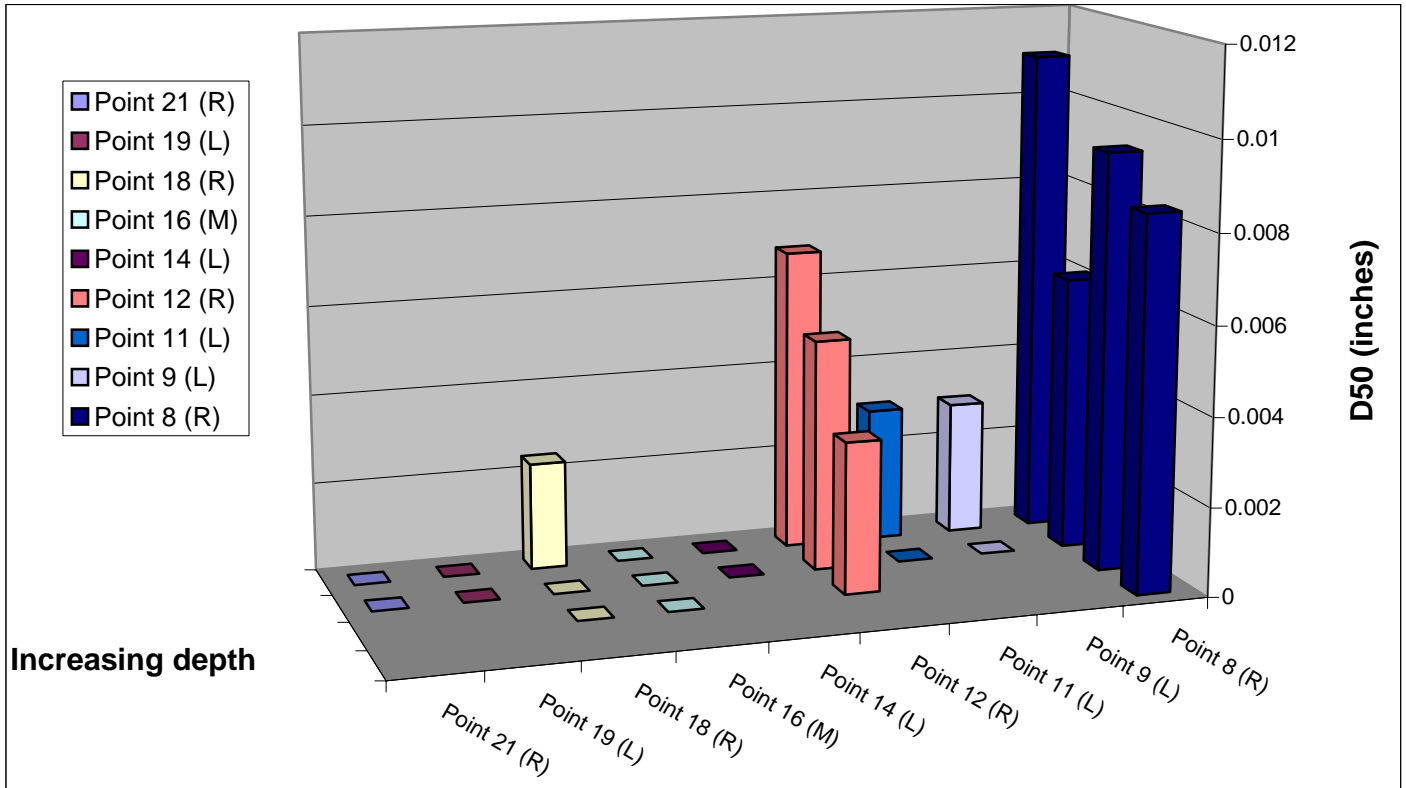


Figure 3.12: D₅₀ of floodplain sediment cores

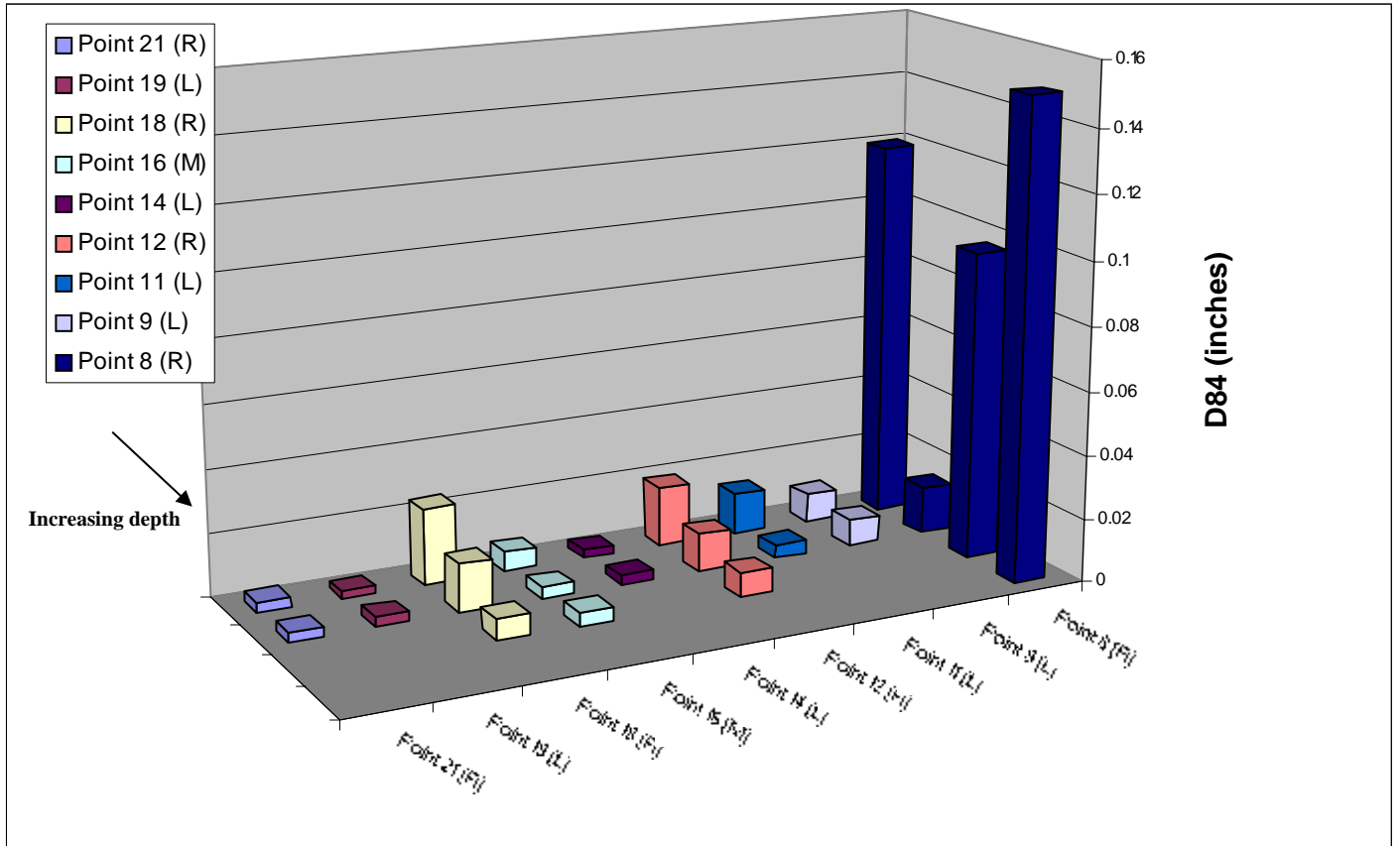


Figure 3.13: D₈₄ of floodplain sediment cores

3.5 – Sediment transport

3.5.1 – Bedload transport

3.5.2 – Suspended load transport

3.5.3 – Comparison of sediment budget to measured sediment transport

3.6 – Pool volumes

The volume of fine sediment contained in the pools downstream from the new culvert is expressed as a dimensionless number, V^* , which is obtained by normalizing the volume of fine sediment by the sum of the volumes of fine sediment and water contained in the scoured residual pool (see section 2.5 for definition). The method for obtaining these volumes is straightforward and involves calculating the volumes of water and sediment between adjacent cross-sections and then summing the results to obtain pool totals. The method is described in detail by [Hilton, 1993 #1267].

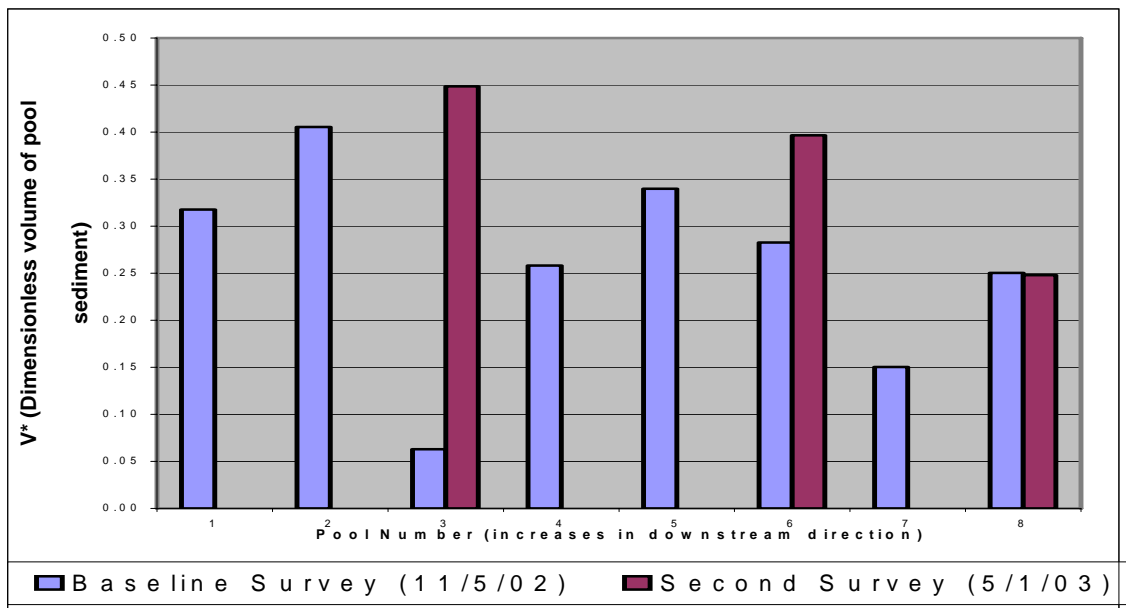


Figure 3.7: Dimensionless sediment volume in pools downstream from the new culvert

Pool No.	Dimensionless Sediment Volume (V*)	
	Baseline Survey (11/5/02)	Second Survey (5/1/03)
1	0.3176	
2	0.4055	
3	0.0628	0.4488
4	0.2582	
5	0.3399	
6	0.2826	0.3967
7	0.1503	
8	0.2504	0.2481
Mean	0.2584	0.3645

Table 3.3: Summary of dimensionless sediment volume (V*)

The results of the analysis are summarized in Table 3.3. Two of the three pools in the second survey show clear increases in the volume of fine sediment (Figure 3.7), while the mean volume of fine sediment has also increased from 0.2584 to 0.3645 between the two surveys. Although the data from the second survey are sparse, this suggests that there has been a net increase in the volume of fine sediment stored in the pools over the winter period.

The pattern of fine sediment volume change from pool to pool is also interesting. The baseline survey shows no clear trend in the downstream direction. The second survey, however, suggests that there may be a decreasing volume of fine sediment with increasing distance downstream. This occurs because the upstream-most pools are the first storage zones encountered by the bedload, which thus preferentially deposits here as opposed to the downstream pools. Although this behavior has been documented in the literature (refs), the second survey data are too spatially limited to confirm this occurrence here.

They are also too temporally limited to describe the movement during the winter of the pool sediments. It is hypothesized that sediment ‘hops’ from pool to pool as it is scoured ([Lisle, 1999 #308]-*need original reference for this observation*), such that the location of maximum sediment pool storage moves steadily downstream. This was observed over the course of several winter storms by [Wohl, 2000 #622] following a reservoir sediment-release into the North Fork Poudre River of Colorado. There are two possibilities, however. The first is that all of the sediment eroded from the incising reach by the high flow events (Figure 3.6) has been stored in the upstream-most pools and that there have been too few storm events to move this sediment into the more downstream pools. The second is that each storm event was able to move the sediment through the downstream system, with minimal pool storage, until the receding flows were no longer able to move the bedload. At this point, the bedload would fall into the pools and not be mobilized until the next high flow event. In this case, the pattern of storage shown in Figure 3.7 represents the sediment that was deposited on the falling limb of the last winter hydrograph.

4.0 Discussion

4.1 – Evolution of the sediment deposit

Description of the evolution of the geometry of impounded sediment; compare this to known way in which incising channels evolve and to channel evolution models ([Schumm, 1984 #12; Simon, 1989 #191]); discuss the unquantified (by this study) role of woody material in the system's evolution. Produce a map to show location of woody material in system and its position relative to the locations of bank scour (construct this map using photographic evidence).

Role of woody debris – not quantified in this study.

- *Calculate equilibrium slope towards which the channel is likely to adjust.*
- *Estimate the length of time that this is likely to take based on the length of time taken thus far for geomorphic work to occur*
- *Need to determine whether or not the above is even a valid approach given that the system appears to be such a cohesive one, i.e. it is not necessarily behaving like a sand or gravel bed channel. It may, however, be very similar to the cohesive boundaries of the incising Mississippi channels – see Andy Simon's stuff to verify this.*

The depth of the valley floor prior to any disturbance in the basin, be this from the construction of Honey Grove Road or from logging, is unknown. It may be that the resistant layer formed by cohesive clay marks this surface. Alternately, this clay layer may have been the result of basin disturbance that mobilized a large volume of fines without mobilizing significant quantities of any coarser fraction. For instance, Honey Grove Road may have been built several decades before the onset of logging in the basin. Storm events may have mobilized fine sediment during this time but, because of the undisturbed vegetation layer, only a negligible amount of coarser material. As this suspended sediment-laden discharge entered the area upstream of the road it formed an impoundment within which the fines were able to settle out of suspension. Over time and with the addition of further sediments, including those mobilized by later logging activity, these fines began to dewater and compact into highly cohesive layer.

The depth of this cohesive layer relative to the pre-project-disturbance floodplain and channel bed elevations in the study reach is presented in Figure 3.14. The channel bed plots (blue) are based on the elevation data from points 7, 13, 17 and 20 (Figure 1.2). The plots for the right side of the study area (red) are based on the elevation data from points 8, 12, 18 and 21, while the plots for the left side of the study area (green) are based on the elevation data from points 9, 11, 14 and 19. The peak in the elevation of the cohesive layer at point 12 occurs because of the presence of buried wood in the floodplain. The true depth of the cohesive later is thus somewhere below this elevation. Allowing for this, the three longitudinal transects through the study area show a general decrease in the depth of the coarser layer overlying the cohesive layer. This is to be expected, since a sediment-transporting flow that enters standing water rapidly loses its energy, which means that it is no longer able to transport its entire sediment load. The coarsest particles are thus deposited first, since these require the greatest energy to transport, while the progressively smaller particles are able to travel progressively further into the standing water before eventually settling out of suspension ([Morris, 1998 #5]). This pattern is thus further evidence that the impounded sediment was deposited into standing water.

Unfortunately, the depth to the cohesive layer is only measured at three points beneath the thalweg within and just upstream of the study reach, but the control that this cohesive layer is exerting on the channel's evolution is nevertheless evident. Figure 4.1 shows the elevation of this layer below the channel thalweg relative to the thalweg and bed slope evolution data presented in Figures 3.4 and 3.5. Upstream of about 5,740 feet on the upstream slope section, the thalweg of the third, fourth and fifth surveys can be seen either impinging directly upon or coming to within two to three inches of the cohesive layer. This suggests that vertical adjustment will be curtailed, or at least greatly slowed, beyond this point. Further downstream in this upstream slope section, the thalweg appears to be a little further above the cohesive layer and it thus still has the ability to adjust vertically.

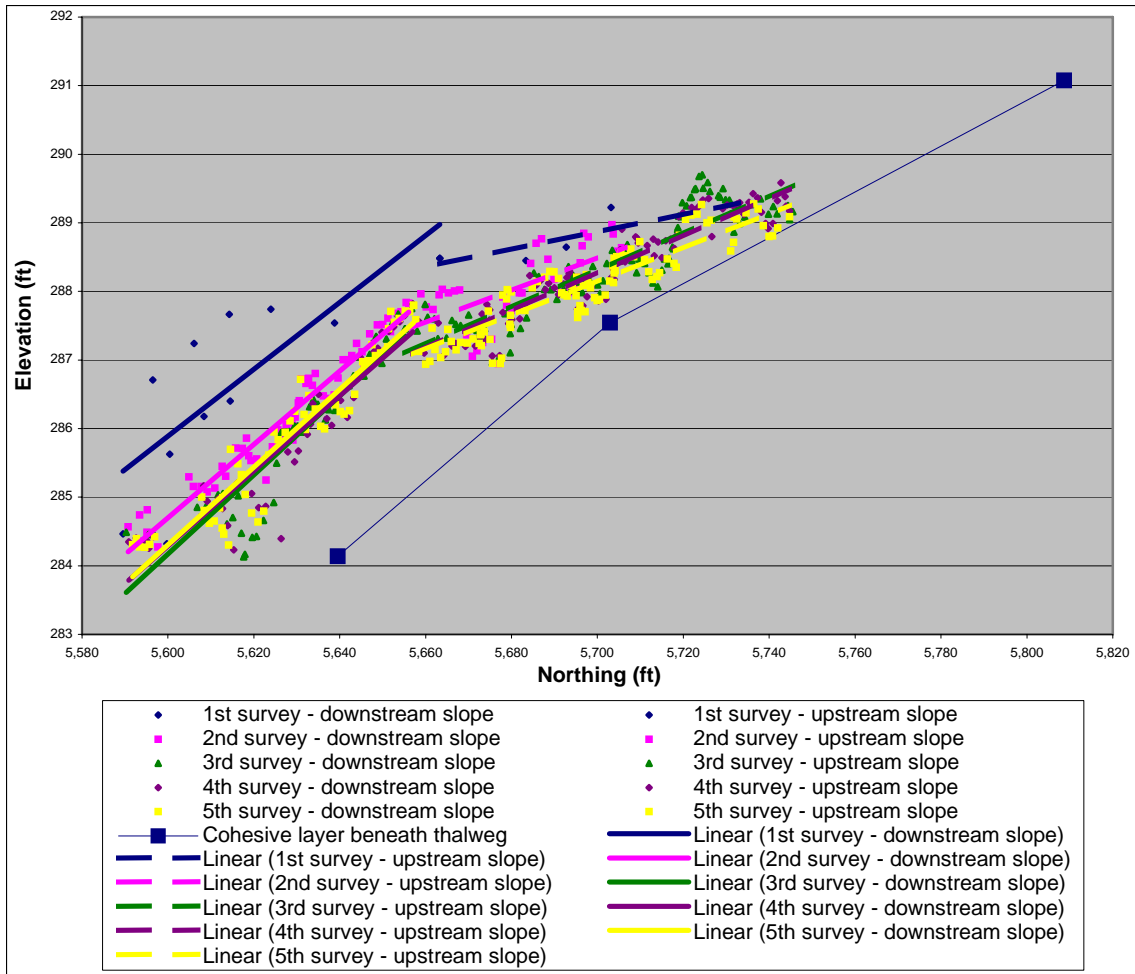


Figure 4.1: Control exerted by the cohesive layer on vertical adjustment in the incising reach

4.2 – Downstream implications of upstream system evolution

A qualitative assessment of the likely downstream impacts of the project. Use pool volume results as much as possible and then the downstream photographs to make qualitative observations.

5.0 Conclusions

The system will continue to evolve for a further number of years; intention to monitor over next winter. Is it possible to make an estimate of the length of time over which the system will continue to evolve? *I.e.* can we calculate what the equilibrium slope should be and how much material needs to be eroded in order to achieve this slope?

6.0 Acknowledgements

? for providing financial support for the monitoring program

Chuck Knoll, Benton County Public Works, for invaluable assistance in developing and executing the monitoring program.

Dawit ? and Mike ? for help with sample and data collection in the field.

? for allowing me to use the facilities in the Central Analytical Laboratory, Department of Crop and Soil Science, Oregon State University.

Sandra Lovelady for TSS analysis

Wa Chang and Associates, ?, Oregon, for the extended loan of the ISCO pumped sampler.

? for reviews of an earlier draft of this report.

7.0 References